Supporting information

Ortho-phenylenediamine-based open and macrocyclic receptors in selective sensing of $H_2PO_4^-$, ATP and ADP under different conditions

Kumaresh Ghosh* and Indrajit Saha

Department of Chemistry,
University of Kalyani, Kalyani-741235, India.
Email: ghosh_k2003@yahoo.co.in, Fax: +913325828282; Tel: +913325828750.

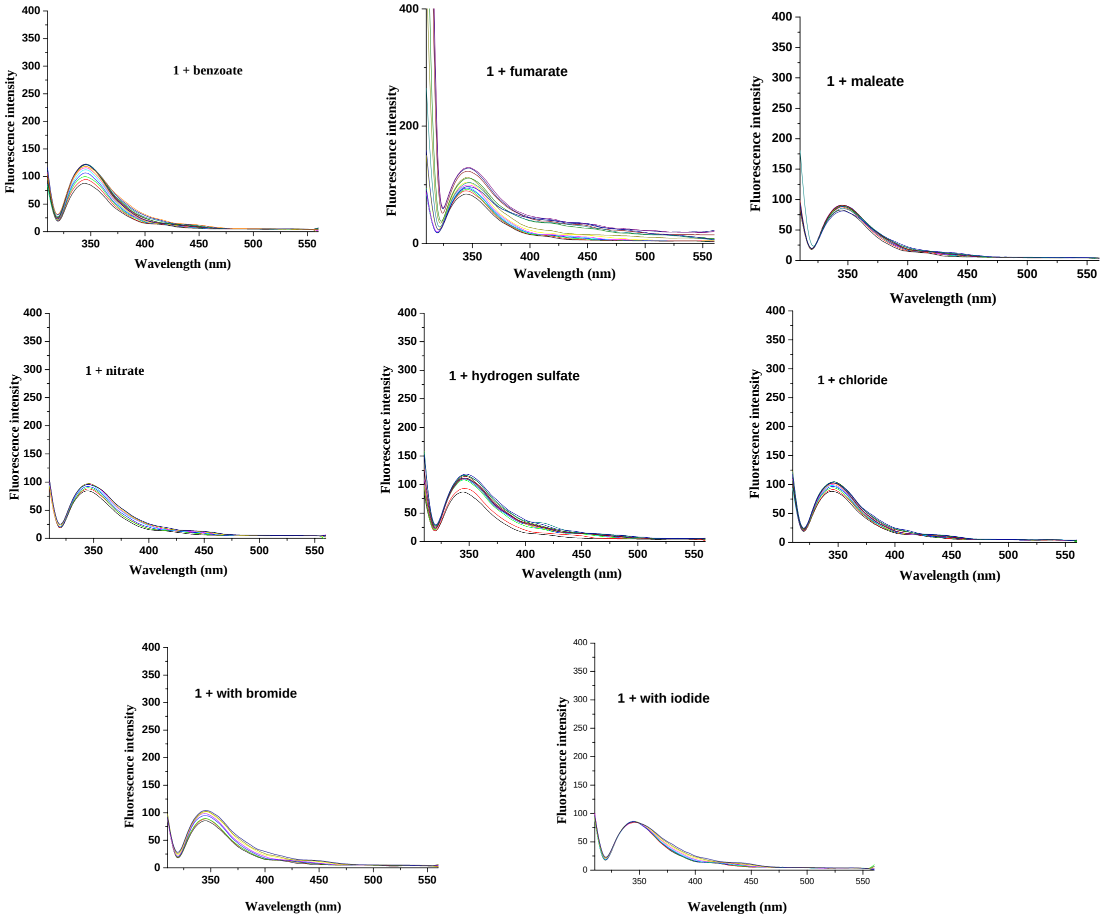

Figure S1. Change in fluorescence intensity of receptor **1** (c = 3.75 x 10^{-5} M) upon addition anions (c = 1.5 x 10^{-3} M) in CH_3CN (λ_{ex} = 300 nm).

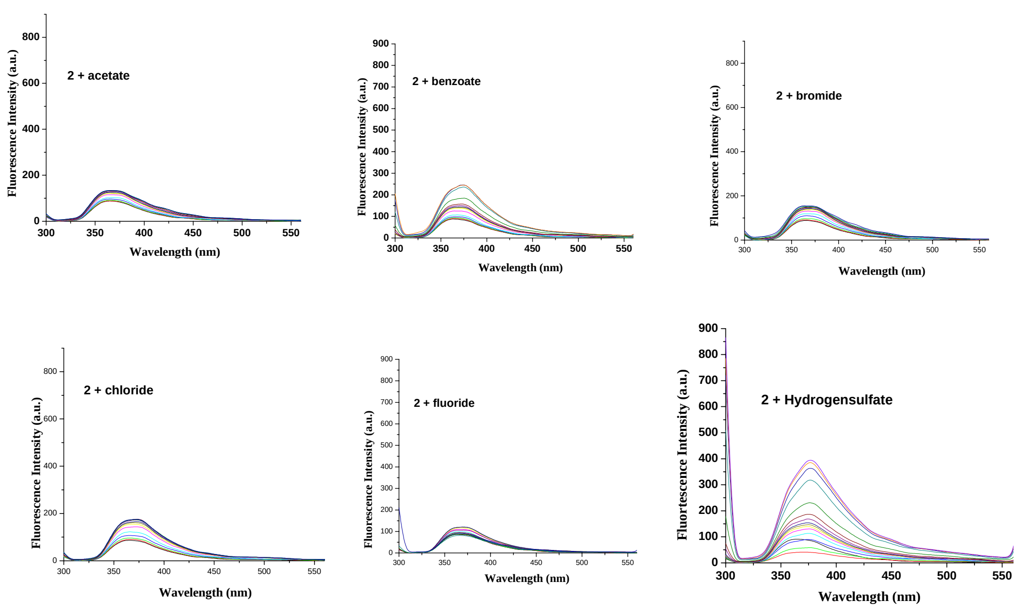

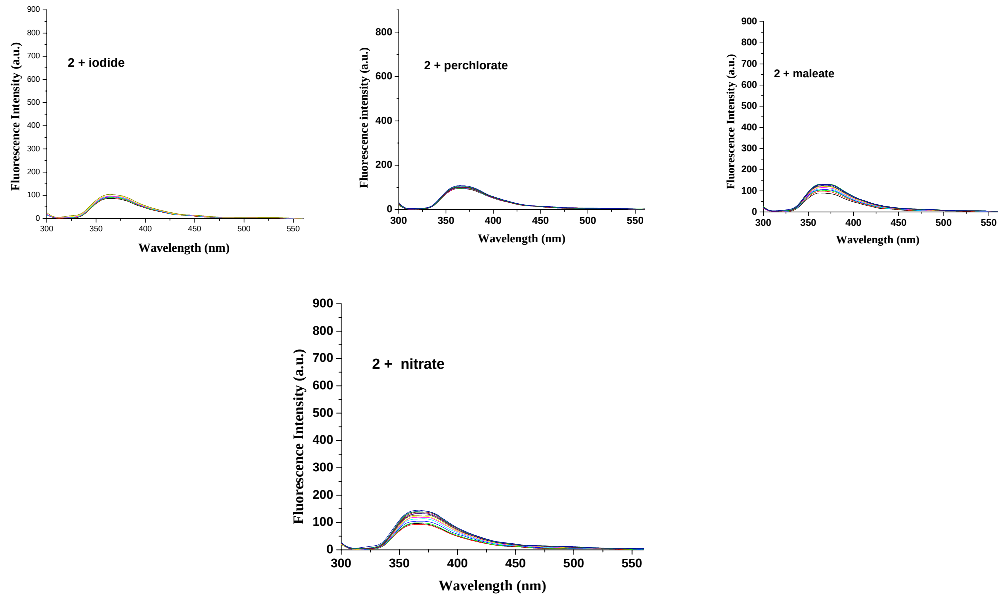

Figure S2. Change in fluorescence intensity of receptor **2** (c = 3.43 x 10^{-5} M) upon addition anions (c = 1.5 x 10^{-3} M) in CH_3CN (λ_{ex} = 300 nm).

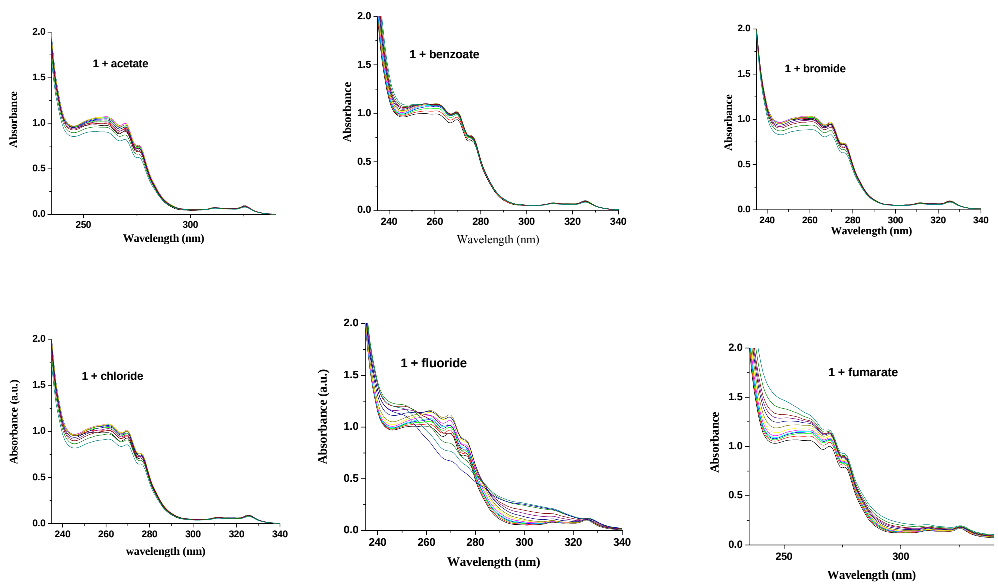

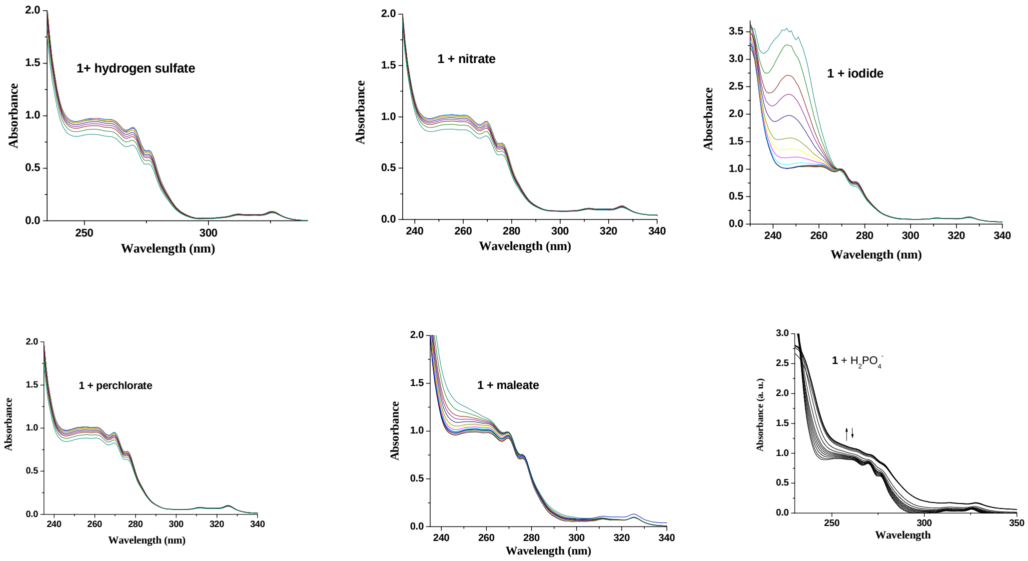

Figure S3. Change in absorbance of receptor **1** (c = 3.75 x 10^{-5} M) upon addition anions (c = 1.5 x 10^{-3} M) in CH_3CN (λ_{ex} = 300 nm).

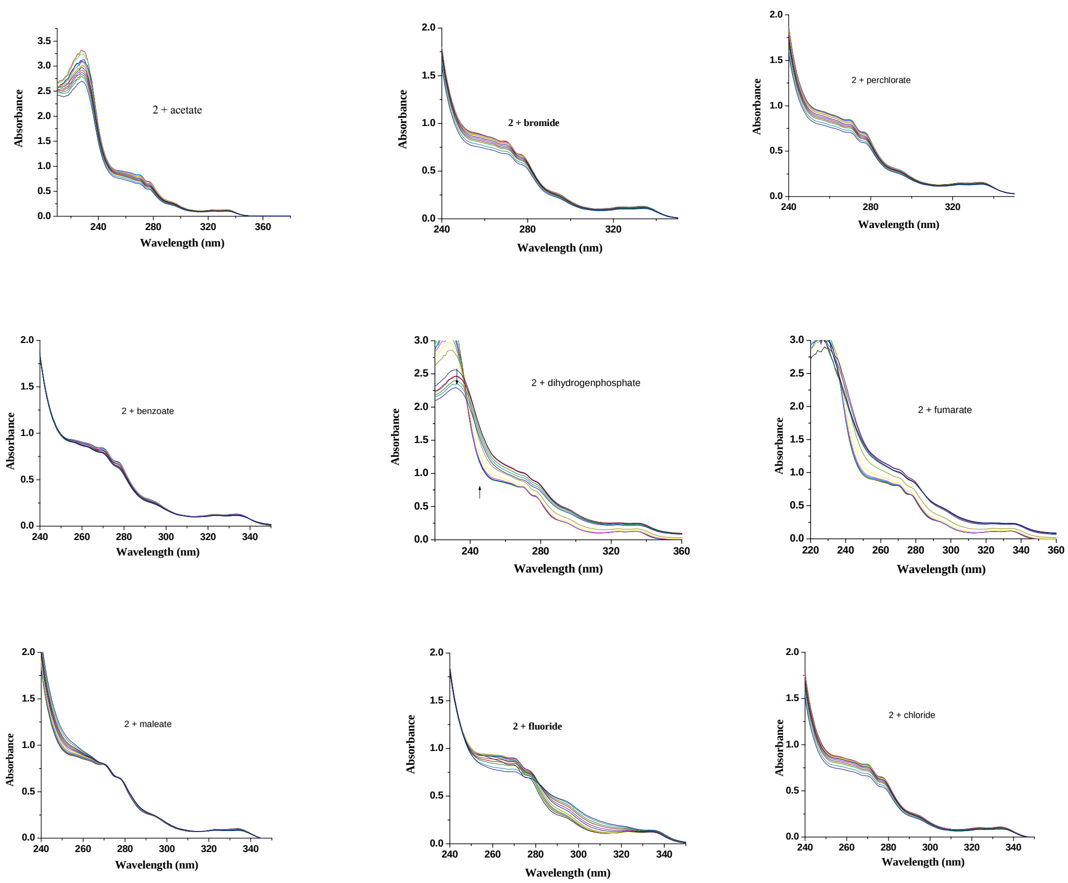

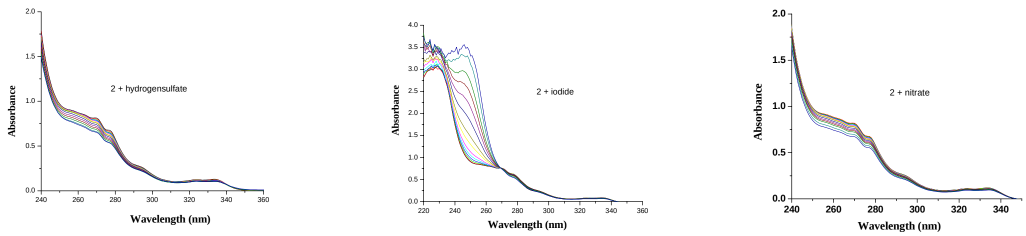

Figure S4. Change in absorbance of receptor **2** (c = 3.43 x 10^{-5} M) upon addition anions (c = 1.5 x 10^{-3} M) in CH_3CN (λ_{ex} = 300 nm).

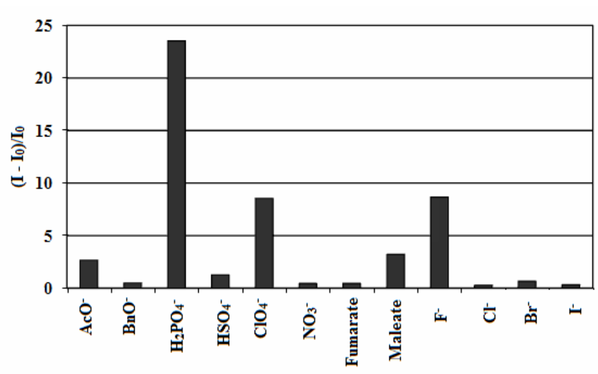

Figure S5. Fluorescence ratio ($I - I_0/I_0$) of receptor **1** (c = 3.75 x 10^{-5} M) at 422 nm upon addition of 10.0 equiv. amounts of a particular anion in CH_3CN.

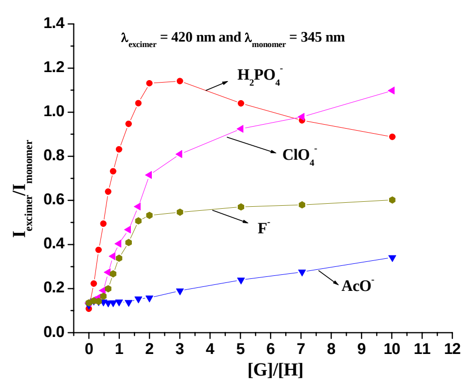

Figure S6. Ratio of excimer to monomer emissions of **1** (c = 3.75 x 10^{-5} M) with increase in concentration of anions in CH_3CN.

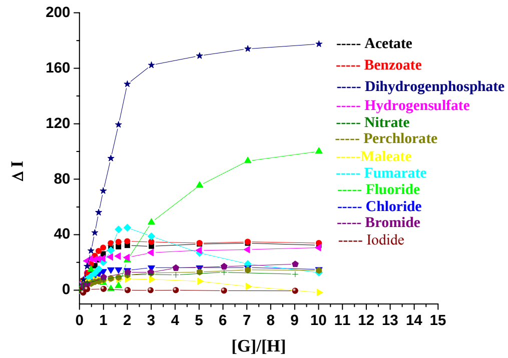

Figure S7. Fluorescence titration curves ([Guest]/[Host] vs change in emission) of **1** (c = 3.75 x 10^{-5} M) measured at 345 nm in CH_3CN.

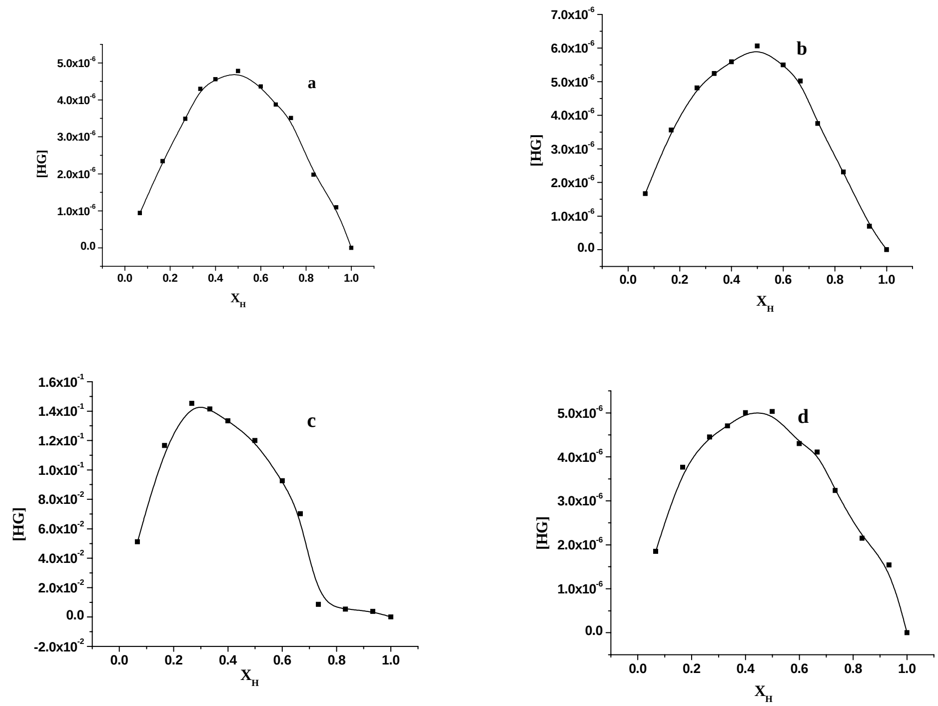

Figure S8. Fluorescence Job plots of receptor **1** (3.97 x 10^{-5} M) with a) $H_2PO_4^-$, b) F^-, c) Fumarate and d) ClO_4^- in CH_3CN.

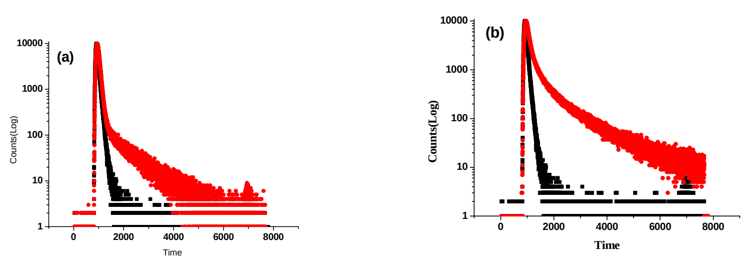

Figure S9. Fluorescence decays of (a) **1** (c = 4.24 x 10^{-5} M) in CH_3CN measured at 345 nm. (λ_{ex} = 300 nm); (b) **1** (c = 4.24 x 10^{-5} M) in the presence of equivalent amount of $H_2PO_4^-$ ions in CH_3CN measured at 345 nm (λ_{ex} = 300 nm).

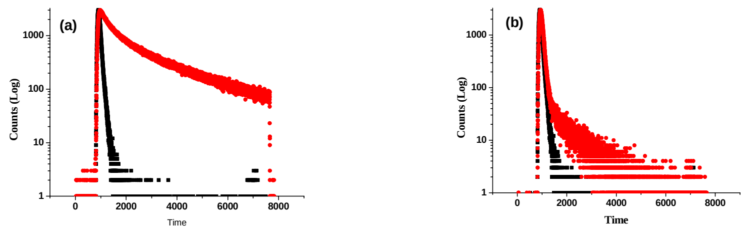

Figure S10. Fluorescence decays of (a) **1** (c = 4.24 x 10^{-5} M) in the presence of equivalent amount of $H_2PO_4^-$ ions in CH_3CN measured at 420 nm (λ_{ex} = 300 nm); (b) **1** (c = 4.24 x 10^{-5} M) in the presence of equivalent amount of ClO_4^- ions in CH_3CN measured at 345 nm (λ_{ex} = 300 nm).

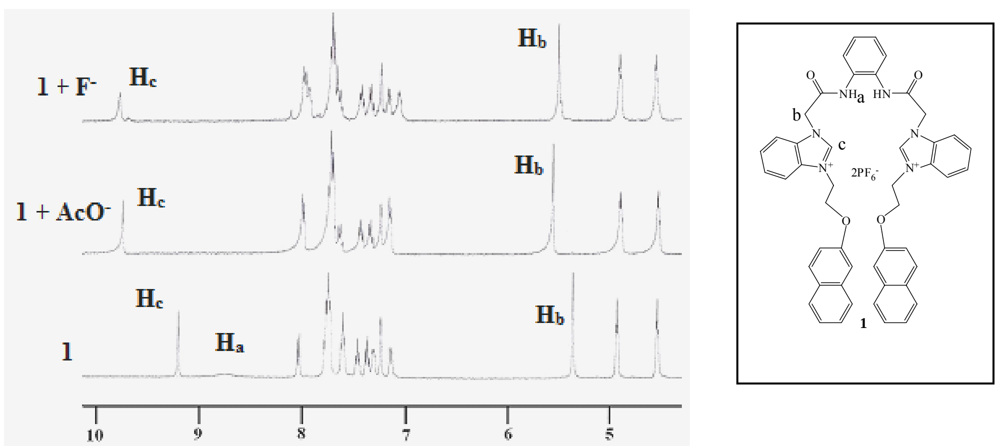

Figure S11. Partial ^1H NMR (CD_3CN, 400 MHz) of **1** (c = 2.65 x 10^{-3} M) with equivalent amount of AcO^- and F^-.

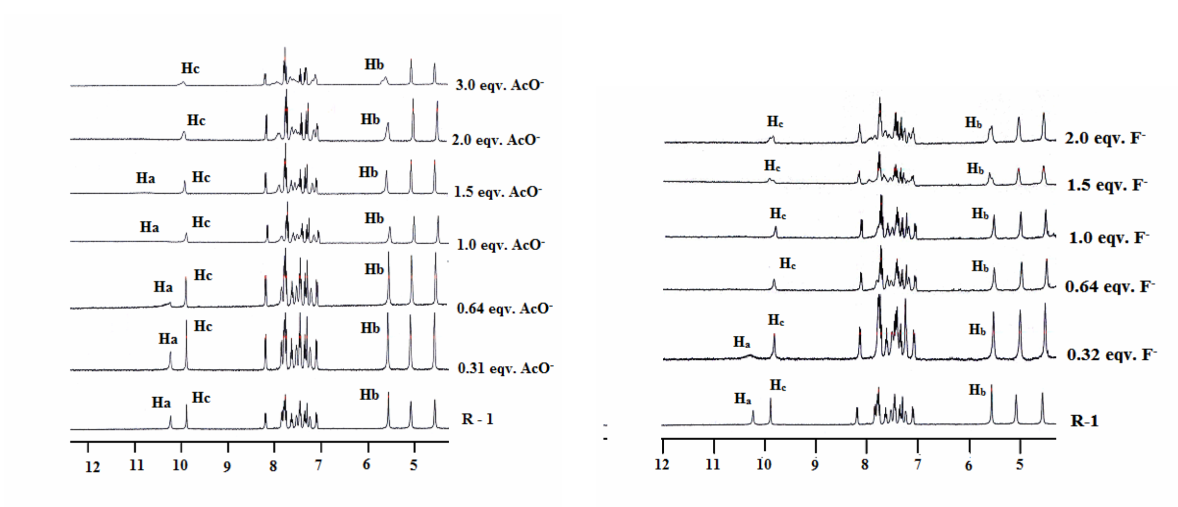

(a) (b)

Figure S12. Change in ^1H NMR (400 MHz) of **1** (c = 2.67 x 10^{-3} M) upon successive addition of tetrabutylammonium (a) acetate, (b) fluoride in d_6-DMSO.

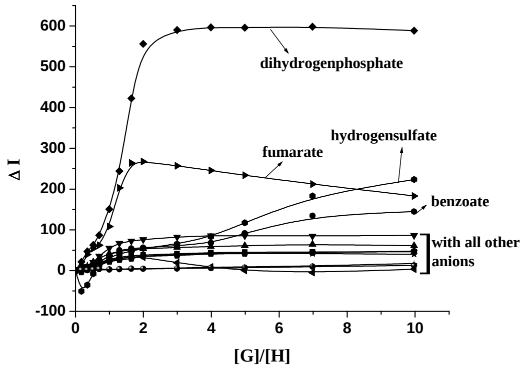

Figure S13. Fluorescence titration curves ([Guest]/[Host] vs change in emission) of **2** (c = 3.43 x 10^{-5} M) measured at 365 nm in CH_3CN.

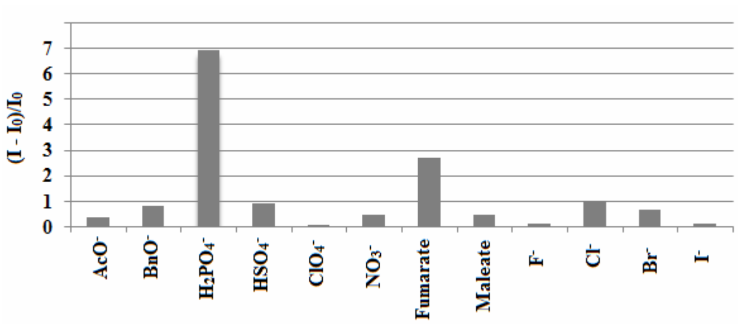

Figure S14. Fluorescence ratio ($I - I_0/I_0$) of receptor **2** (c = 3.43 x 10^{-5} M) at 365 nm upon addition of 4.0 equiv of a particular anion in CH_3CN.

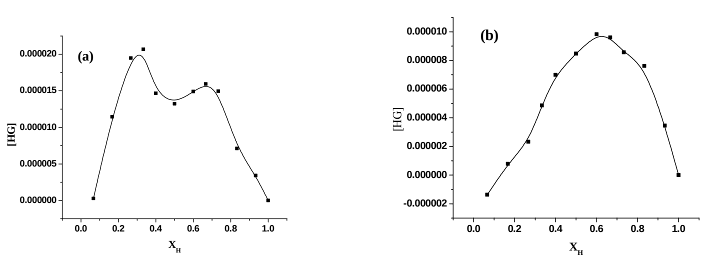

Figure S15. Fluorescence Job plots of receptor **2** (4.42 x 10^{-5} M) with (a) $H_2PO_4^-$ and (b) fumarate in CH_3CN.

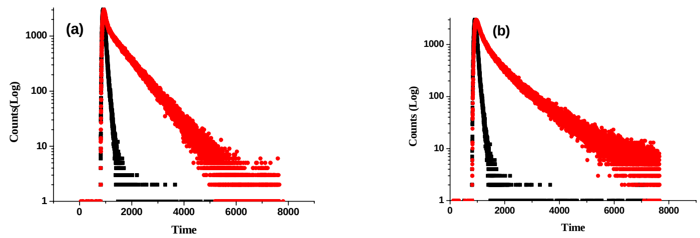

Figure S16. Fluorescence decays of (a) **2** (c = 2.88 x 10^{-5} M) and (b) **2** (c = 2.88 x 10^{-5} M) in the presence of equivalent amount of $H_2PO_4^-$ ions in CH_3CN measured at 365 nm (λ_{ex} = 300 nm).

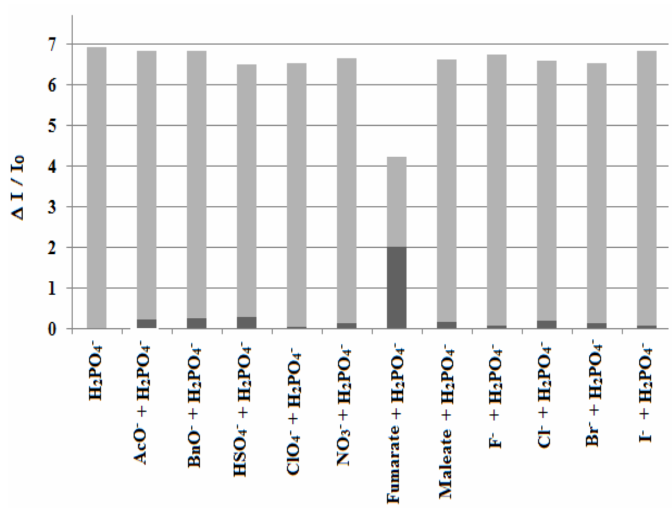

Figure S17. Change in fluorescence ratio of receptor **2** (c = 3.43 x 10^{-5} M) upon addition of 10 equivalent amounts of $H_2PO_4^-$ in the presence of other anions in CH_3CN.

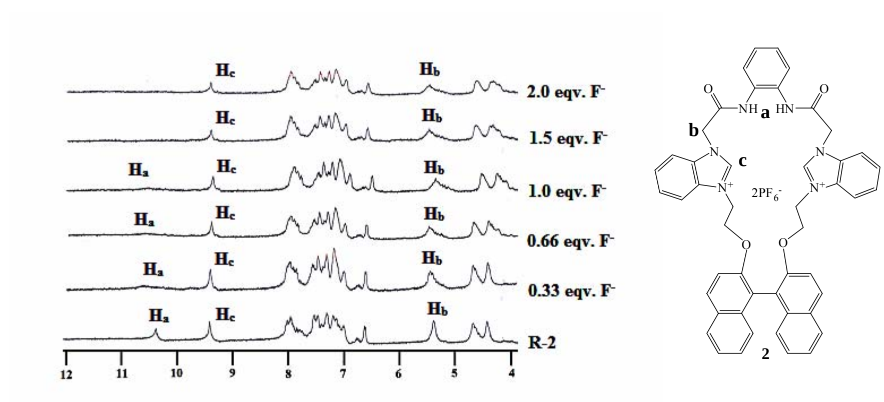

Figure S18. Change in [1]H NMR (400 MHz) of **2** (c = 2.85 x 10^{-3} M) upon successive addition of tetrabutylammonium fluoride in d_6-DMSO.

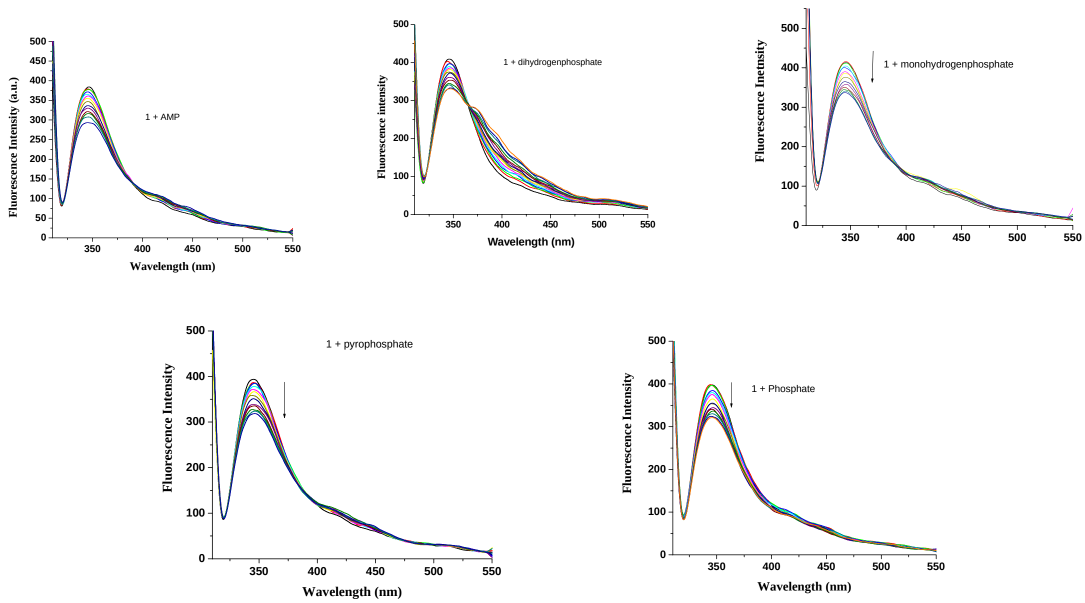

Figure S19. Change in emission of receptor **1** (c = 4.92 x 10^{-5} M, λ_{ex} = 300 nm, slit ex/em = 9/11, λ_{max} = 345 nm, filter = open) upon addition of various anions in CH_3CN: H_2O (1:1, v/v).

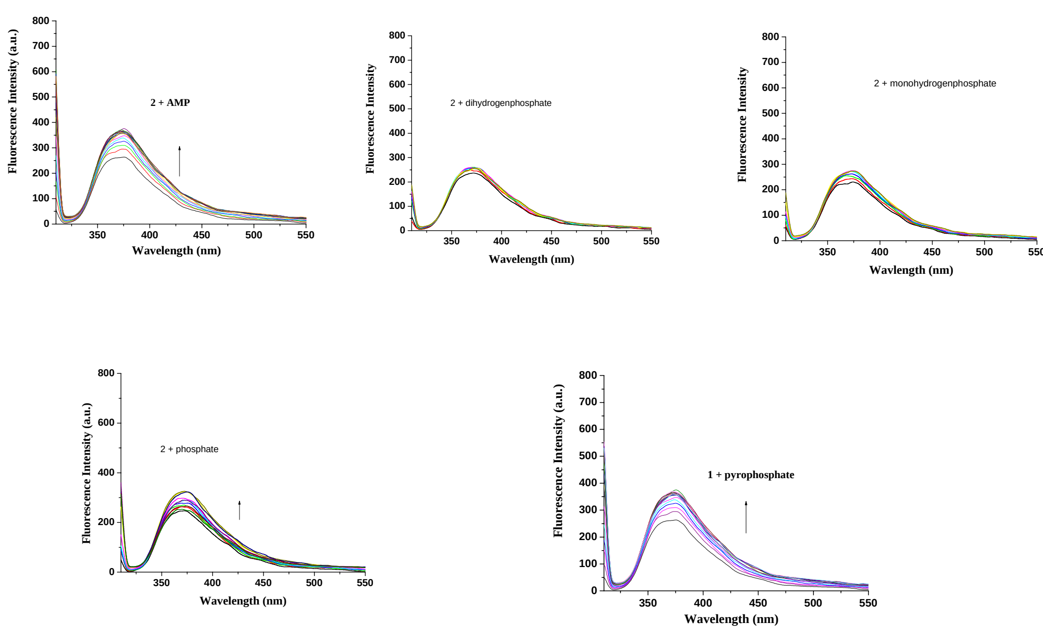

Figure S20. Change in emission of receptor **2** (c = 3.83 x 10^{-5} M, λ_{ex} = 300 nm, slit ex/em = 9/11, λ_{max} = 345 nm, filter = open) upon addition of various anions in CH_3CN: H_2O (1:1, v/v)

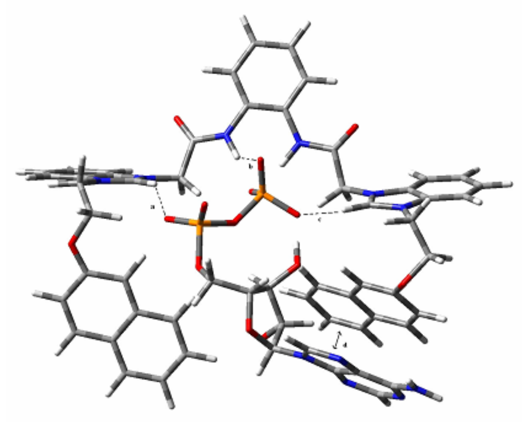

Figure S21. PM6 optimized structure for **1** with ADP (a = 2.06 Å, b = 1.77 Å, c = 1.71 Å, d = 2.17 Å) in CH_3CN.

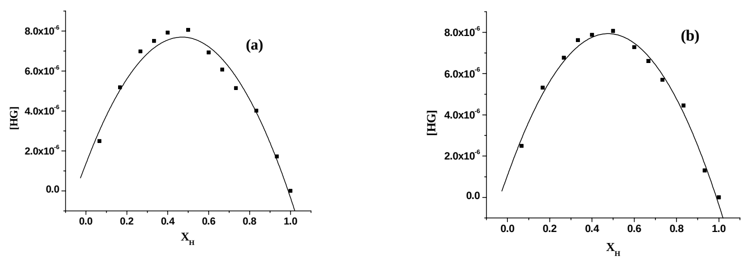

Figure S22. Fluorescence Job plots of receptor **1** (c = 5.32 x 10^{-5} M) with (a) ADP and (b) ATP in CH_3CN: H_2O (1:1, v/v).

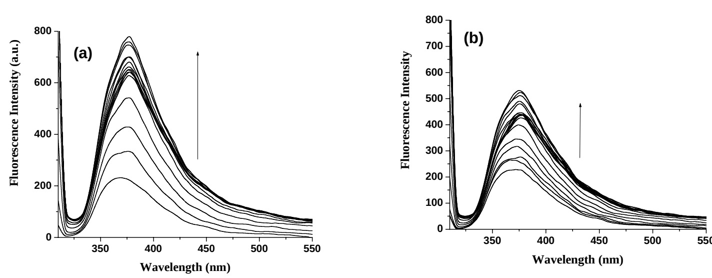

Figure S23. Change in emission of receptor **2** (c = 3.83 x 10^{-5} M) with increase in concentrations of (a) ATP and (b) ADP upon excitation at 300 nm in CH_3CN/ H_2O (1:1, v/v).

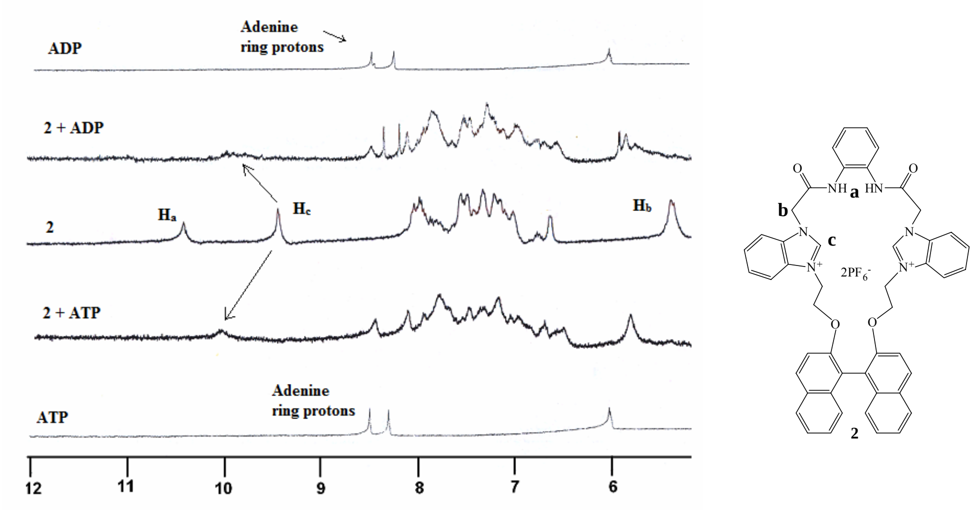

Figure S24. Partial ^{1}H NMR (DMSO -d_6, 400 MHz) of **2** (c = 2.65 x 10^{-3} M) with equivalent amount of ATP and ADP.

Electronic Supplementary Material (ESI) for Organic & Biomolecular Chemistry

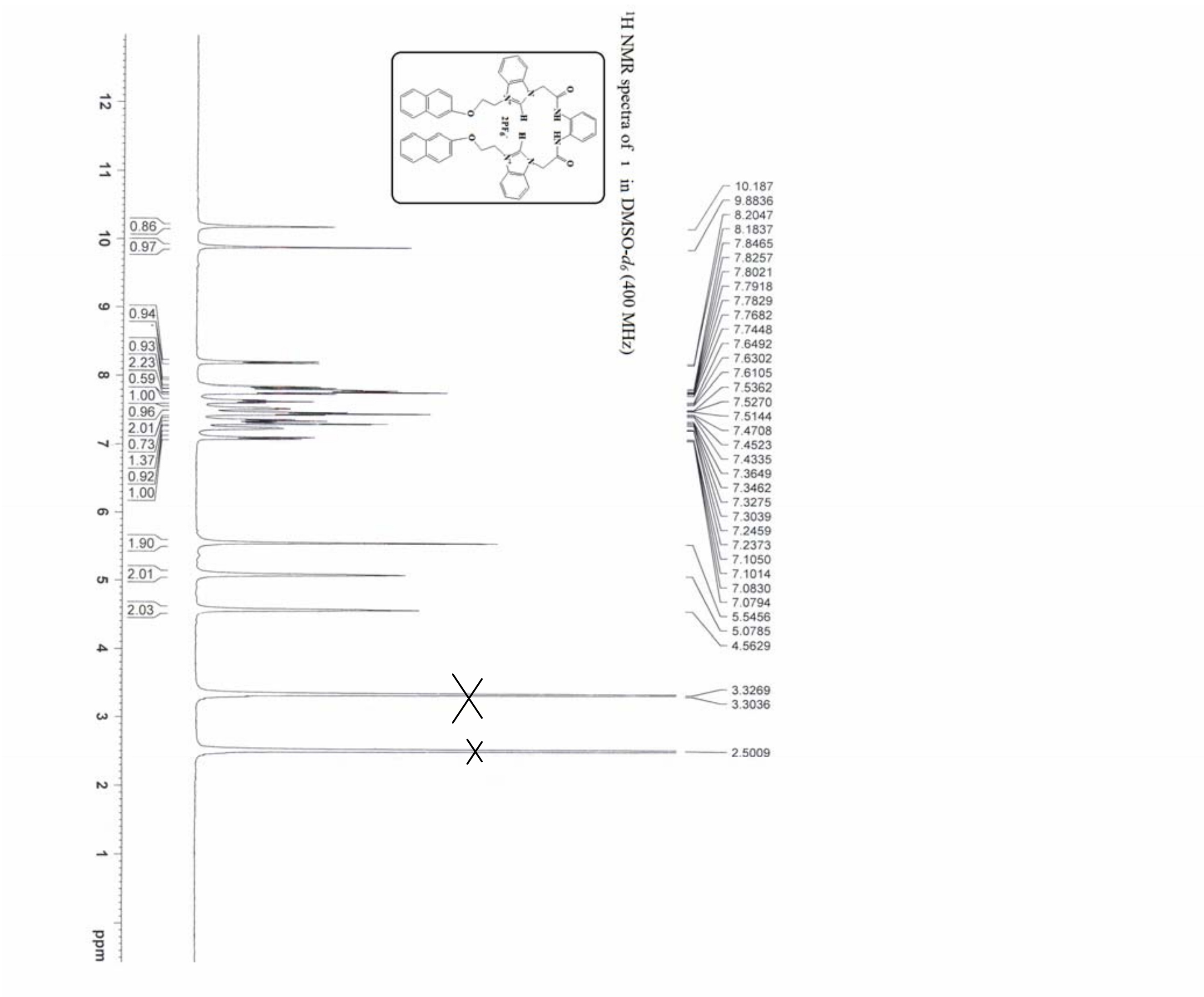

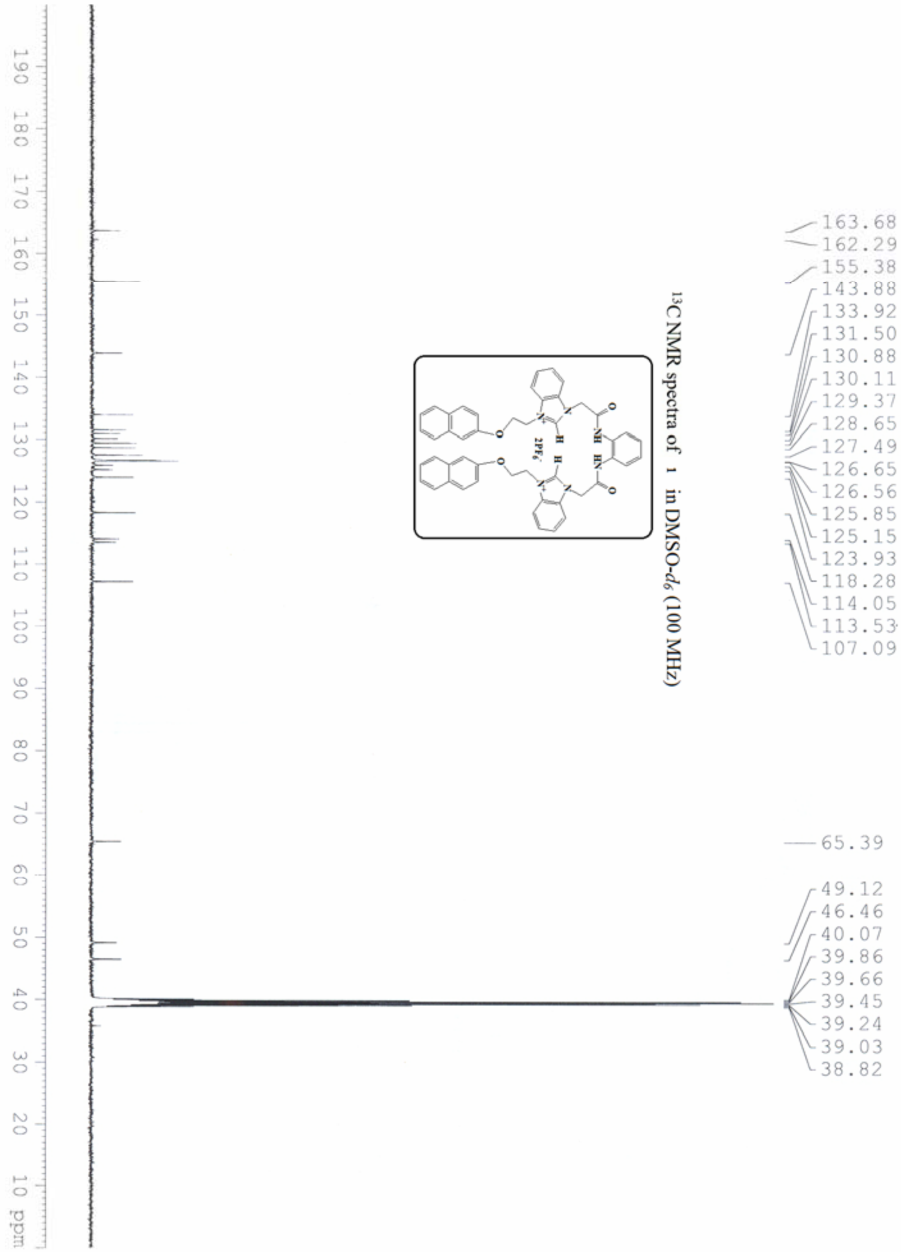

^{13}C NMR spectra of 1 in DMSO-d_6 (100 MHz)

Electronic Supplementary Material (ESI) for Organic & Biomolecular Chemistry

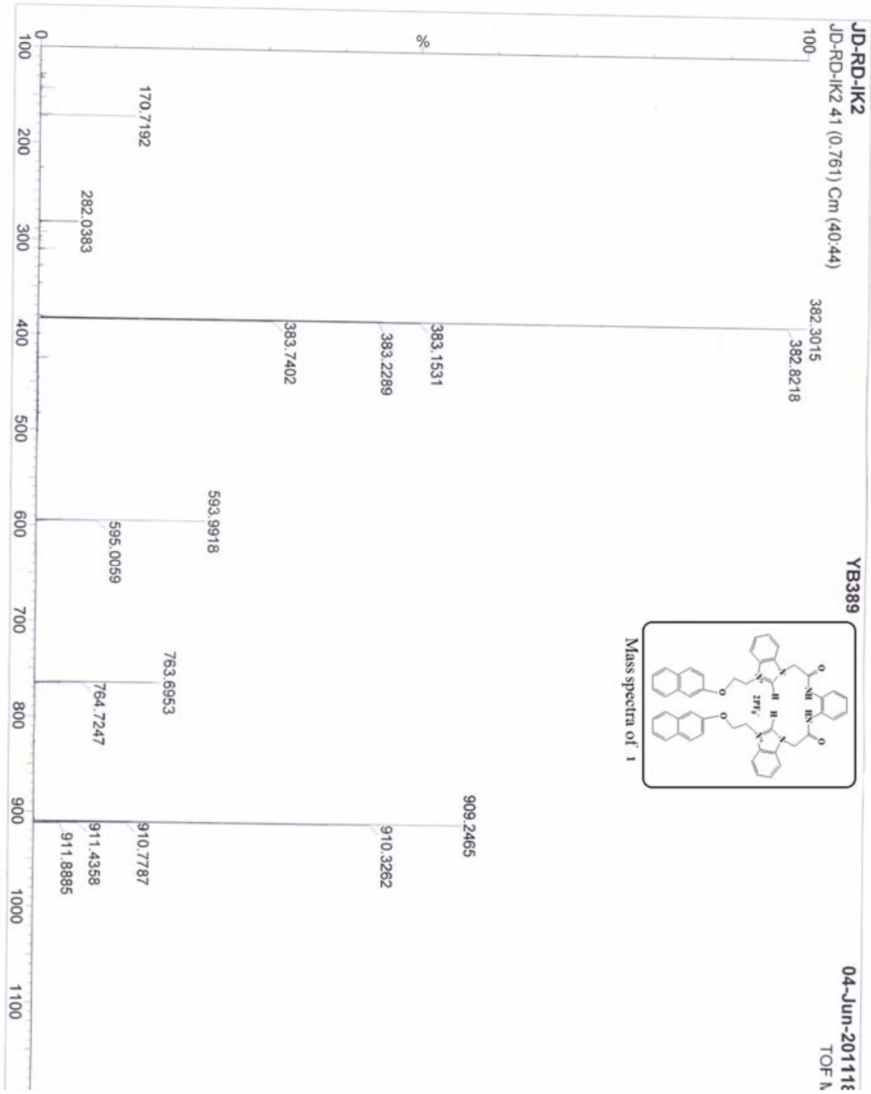

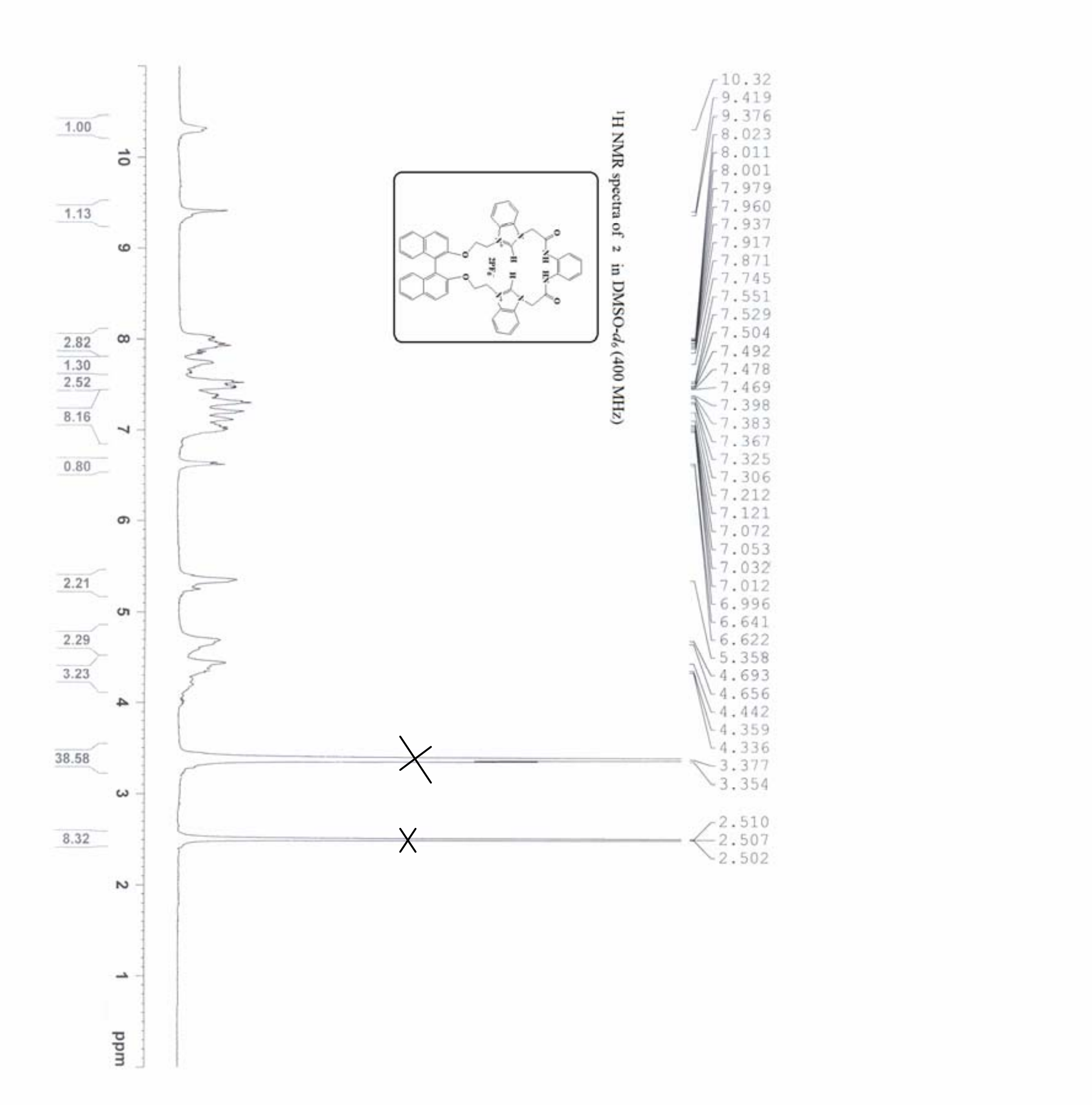

1H NMR spectra of 2 in DMSO-d6 (400 MHz)
2PF6
ppm
1.00
1.13
2.82
1.30
2.52
8.16
0.80
2.21
2.29
3.23
38.58
8.32
10.32
9.419
9.376
8.023
8.011
8.001
7.979
7.960
7.937
7.917
7.871
7.745
7.551
7.529
7.504
7.492
7.478
7.469
7.398
7.383
7.367
7.325
7.306
7.212
7.121
7.072
7.053
7.032
7.012
6.996
6.641
6.622
5.358
4.693
4.656
4.442
4.359
4.336
3.377
3.354
2.510
2.507
2.502

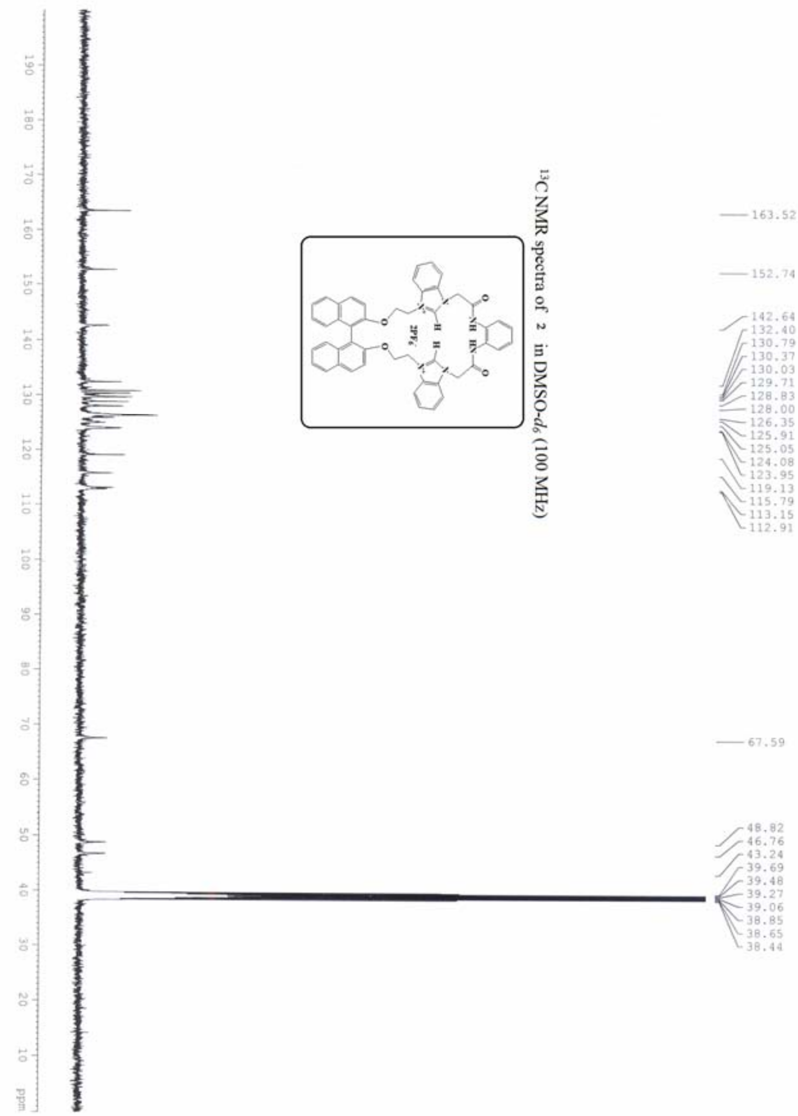

^{13}C NMR spectra of **2** in DMSO-d_6 (100 MHz)

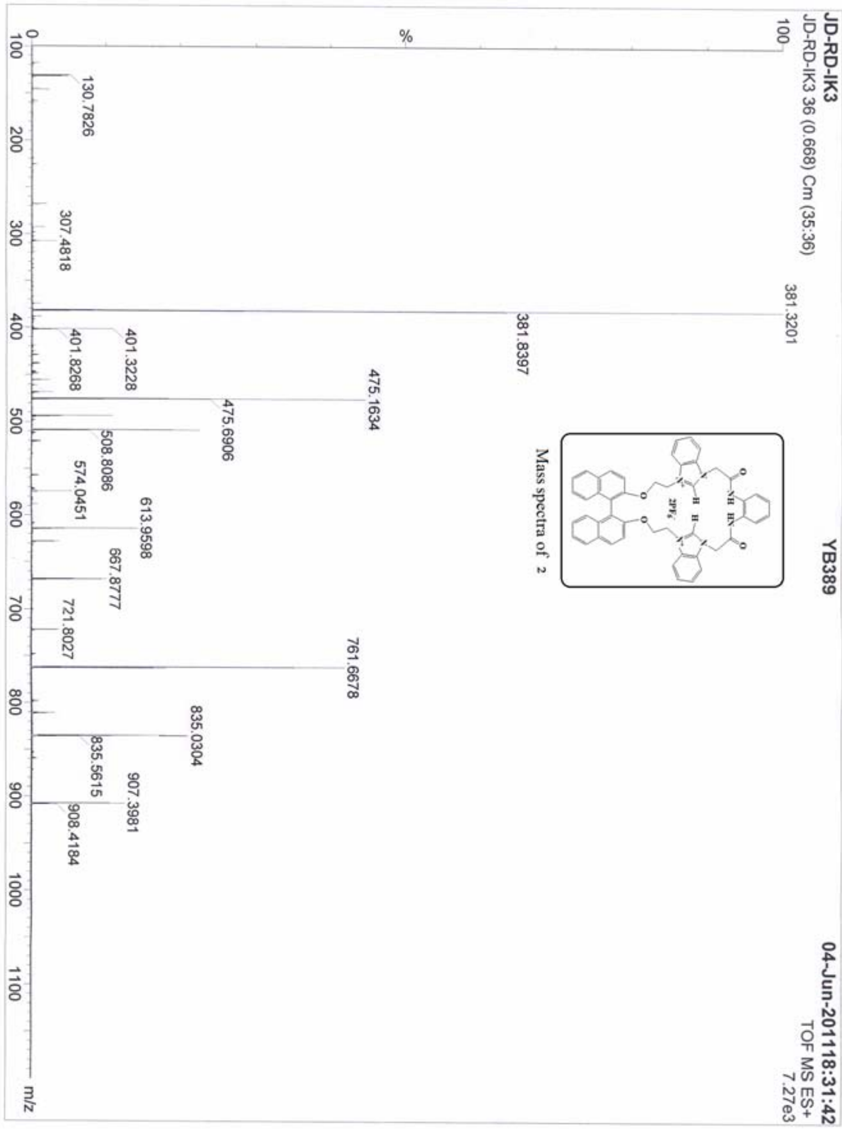
JD-RD-IK3
JD-RD-IK3 36 (0.668) Cm (35:36)
YB389
04-Jun-201118:31:42
TOF MS ES+
7.27e3
Mass spectra of 2
381.3201
381.8397
475.1634
475.6906
761.6678
835.0304
130.7826
307.4818
401.3228
401.8268
508.8086
574.0451
613.9598
667.8777
721.8027
835.5615
907.3981
908.4184
m/z
%